Acta Cryst. (1984). A**40**. 696-701

Lattice Dynamics and Thermal Crystallographic Parameters in Phenothiazine

BY A. CRIADO,* A. CONDE AND R. MÁRQUEZ

Departamento de Optica y Sección de Física del Centro Coordinado del CSIC, Universidad de Sevilla, Spain

(*Received* 12 *March* 1984; *accepted* 18 *June* 1984)

Abstract

A computer program has been developed to study the lattice dynamics of molecular crystals in the harmonic approximation with the external Born–von Kármán formalism and an atom–atom potential function. Dispersion curves are obtained for monoclinic phenothiazine together with frequency distribution functions and external mode contribution to thermodynamic functions. Lattice dynamical **T**, **L** and **S** rigid-body tensors are obtained and individual thermal tensors are compared with experiment. The disagreement with respect to experimental results is of the same order as the disagreement with a Schomaker–Trueblood fit of experimental data.

Introduction

Lattice dynamics in molecular crystals has been the subject of increasing investigations in the past years, and recently has advanced a great deal with the availability of neutron inelastic scattering experiments. As a result a greater amount of experimental data is at our disposal for comparison with theoretical dynamical model calculations. In conjunction with crystallography, lattice-dynamical calculations are an alternative way to obtain atomic mean-square vibration tensors, which are also obtained in the crystal structure analysis process. Here very good results have been obtained by using a potential function model for the crystal of a sum of atom–atom interactions, especially for aromatic hydrocarbons, where atom–atom potential functions, involving C and H atoms, are best established. In this paper we perform a lattice-dynamical calculation of thermal crystallographic parameters of a substance where atoms different from C and H are present, though as a minor part.

In a previous paper (Estrada, Conde & Márquez, 1983) we applied successfully the atom–atom device to the study of the theoretical equilibrium configuration of phenothiazine crystals by means of crystal packing-energy calculations and, as a logical step, we have extended the method to the study of the lattice dynamics of these crystals. This is not a trivial step since lattice dynamics requires more restrictive conditions than those of merely reproducing the experimental crystal structure and therefore proper results are not guaranteed *a priori*.

Method of calculation

Lattice-dynamics vibrational modes for molecular crystals where the rigid-molecule hypothesis is valid are obtained in a straightforward way within the harmonic approximation, *i.e.* small molecular displacements. Here the external Born–von Kármán formalism can be applied by considering each molecule as a solid with six degrees of freedom: three translations and three rotations, arriving at the eigenvalue equation (Born & Huang, 1954)

$$D(\mathbf{q})\mathbf{U}(\mathbf{q}) = \omega^2(\mathbf{q})\mathbf{U}(\mathbf{q}),$$

where these modes are plane waves with angular frequency ω and wave vector $\mathbf{q}$. The amplitude vector $\mathbf{U}$ has $6Z$ components and is complex in general, Z is the number of molecules in the unit cell. $D(\mathbf{q})$ is the dynamical matrix, with dimensions $6Z \times 6Z$, and whose elements can be written explicitly as

$$D^{ii'}_{\alpha\beta}(\mathbf{q}|kk') = \{m^i_\alpha(k)m^{i'}_\beta(k')\}^{-1/2} \times \sum_{l'} \varphi^{ii'}_{\alpha\beta}(lk, l'k') \exp\{i\mathbf{q}[\mathbf{x}(l'k') - \mathbf{x}(lk)]\},$$

where k and k' label the different molecules in the unit cell, i and i' mean either translational or rotational displacements, α and β stand for x, y, z components referred to the molecular principal axes of inertia and $m^i_\alpha(k)$ is the mass of the molecule k or the principal inertia moment I_α; $\mathbf{x}(lk)$ is the position vector of the centre of mass of molecule k in the unit cell l and $\varphi^{ii'}_{\alpha\beta}(lk, l'k')$ represents the tensor of force constants whose components are the second derivatives of the potential energy of the crystal with respect to the molecular displacements $u^i_\alpha(lk)$ and $u^{i'}_\beta(l'k')$ of molecules k and k', each referred to its own principal axes.

In order to perform this study we have written a Fortran program following the method of Pawley (1972), within the harmonic approximation, in which, from the crystal structure and using a pairwise potential model, force constants are calculated analytically as a function of rotational and translational coordinates. 'Self-terms', *i.e.* force constants relating two displacements belonging to the same molecule, can

* This work forms part of the doctoral thesis submitted to the Universidad de Sevilla.

0108-7673/84/060696-06$01.50

also be obtained analytically, but a slight modification in the formulae is necessary (Chaplot, Sahni & Rao, 1981) to take into account second-order rotational displacements when obtaining atomic displacements, so we have maintained its calculation from the invariance conditions (Venkataraman & Sahni, 1970), which are known to give correct results if the crystal structure satisfies the equilibrium conditions for the chosen pairwise potential function (Neto & Kirin, 1979). Once the force constants are known the program constructs the dynamical matrix for any desired wave vector inside the Brillouin zone, whose diagonalization with an extension of the Householder procedure to hermitian matrices (Pawley, 1970) gives us the vibrational frequencies and the wave amplitudes or polarization vectors.

Potential energy functions

The potential energy of the crystal is assumed to be the sum of atomic pair contributions, each pair formed with atoms belonging to different molecules. A central energy functional form is adopted for every pair, in a Buckingham form: $V(r) = -A/r^6 + B\exp(-Cr)$. Here A, B and C are constants, empirically adjustable, and depending on the chemical nature of the atoms involved. In order to reduce the number of independent parameters, it is customary to use combination laws for parameters of mixed interactions, such as the geometric-mean law for attractive and repulsive terms separately (Mason & Rice, 1954). Nevertheless, as pointed out by Mirskaya (1973), it is more correct to establish the geometric mean law for the whole interaction energy, leading to different combination rules. We have maintained the geometric law for A; the arithmetic law for C and B has been adjusted in order to obtain the arithmetic mean for the position of minimum energy. This method yields potential curves which are very close to those of Mirskaya, with the advantage of allowing the use of Williams (1971) convergence methods for lattice sums.

Application to phenothiazine

We have centred our attention on the monoclinic modification of phenothiazine, space group $P2_1$, $a = 7{\cdot}82\,(3)$, $b = 5{\cdot}93\,(1)$, $c = 10{\cdot}70\,(8)$ Å, $\beta = 105{\cdot}99°$ (Bell, Blount, Briscoe & Freeman, 1968) and two molecules per unit cell. A great variety of potential parameters are available in the literature to describe the interactions of C and H atoms. We have selected set IV*a* of Williams (1967) which has been used successfully for obtaining thermal crystallographic parameters in aromatic hydrocarbons (Filippini, Gramaccioli, Simonetta & Suffritti, 1973; Gramaccioli & Filippini, 1983). We have also tested Williams (1972) parameters and Mirskaya, Kozlova & Bereznitskaya (1974) parameters; even though both of them predicted an equilibrium configuration as close to the experimental one as the first set, calculated thermal parameters were slightly worse for the Williams (1972) set, and rather worse (some diagonal thermal parameters twice their experimental values) for the Mirskaya *et al.* parameters, indicating that lattice-dynamics calculations are more critical with respect to potential parameters than packing calculations. For N and S atoms few sets are available in the literature and their transferability to a wide range of compounds is not well established. Nevertheless, in our case, from 284 intermolecular contacts less than 4 Å, only 21 involve S and N atoms (the shortest contact distances are: S···N 3·703, S···C 3·491, S···H 3·185, N···C 3·767 and N···H 3·122 Å) and their importance is expected to be small. We have selected Mirskaya & Nauchitel (1971, 1972) parameters for S and N atoms, which are recommended by Mirsky (1978) because they fulfil the necessary requirements about intermolecular distances, sublimation heats *etc.* All potential parameters are shown in Table 1, where we observe that the equilibrium distances are larger than the sum of the corresponding van der Waals radii, but it is known that atoms in molecular crystals are compressed with respect to their free state and it is the distance at which the energy is zero (when the slope of the curve, *i.e.* the repulsive force, attains a large value) rather than the minimum-energy distance, the magnitude of which is approximately equal to the sum of the van der Waals radii.

The C—H experimental bond lengths were normalized to a value of 1·09 Å, and the corresponding experimental values were kept constant for angles involving hydrogen. Before obtaining frequencies a process of energy minimization was considered to be necessary for this purpose. The program *WMIN* (Busing, 1972) has been used. A translation of molecular mass centre of 0·05 Å and a rotation of 1·4 Å starting from the experimental structure is sufficient to reach the equilibrium and constitutes a first test of the goodness of the potential functions. A cut-off energy distance has been used in order to save computational time and a value of 6 Å has been chosen as enough to ensure stability in packing and dynamical results.

The Brillouin zone (BZ) for monoclinic phenothiazine (Bradley & Cracknell, 1972) is shown in Fig. 1 and the dispersion curves obtained for the binary symmetry direction Λ are shown in Fig. 2.

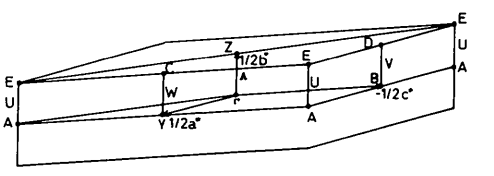

Fig. 1. Brillouin zone for monoclinic phenothiazine.

Table 1. *Potential parameters*

$V(r) = -A/r^6 + B\exp(-Cr)$.

σ is the zero energy distance, r_0 the minimum energy distance and ε_m the minimum energy value.

Interaction	A(kJ bond^{-1} Å^6) ($\times 10^{23}$)	B(kJ bond^{-1}) ($\times 10^{23}$)	C(Å^{-1})	σ(Å)	r_0(Å)	ε_m (J bond^{-1}) ($\times 10^{23}$)
C···C	22·63	3332·9	3·60	3·45	3·88	−3·78
C···H	4·96	349·3	3·67	2·90	3·30	−1·91
H···H	1·08	105·8	3·74	2·97	3·37	−0·35
N···N	10·32	1673·9	3·78	3·19	3·59	−2·78
S···S	93·49	9365·6	3·49	3·45	3·88	−15·14
C···N	15·28	2370·5	3·69	3·32	3·73	−3·14
C···S	46·00	5435·5	3·54	3·44	3·88	−7·57
H···H	3·35	259·5	3·76	2·80	3·19	−1·55
H···S	10·08	623·2	3·61	2·93	3·34	−3·62
N···S	31·06	3914·6	3·63	3·31	3·73	−6·37

Along this direction, and as a result of group theory, two representations are allowed and the branches can be labelled as S or A, indicating a symmetric or antisymmetric character with respect to the rotation axis, and at the zone frontier, $\mathbf{q} = \pi\mathbf{b}^*$ pairs of S and A branches coincide because of the temporal inversion symmetry, the frequencies being degenerate at this point. Of these 12 branches three are acoustic, with $\omega = 0$ for $q = 0$.

Frequency distribution functions can be obtained by performing dense sampling inside the Brillouin zone. In our case we have chosen a division of each reciprocal basis vector into 24 parts and a frequency channel of 1 cm^{-1} for a histogram representation. Sampling has been reduced to the irreducible part of the BZ (3456 points) and the total external mode contribution, together with the translational and rotational contributions, are shown in Figs. 3, 3(a) and 3(b).* An important translational contribution is observed at low frequencies due to the acoustic modes; on the contrary, at high frequencies the most important contribution is rotational, although in neither case are there purely translational or rotational modes. The Debye parabolic approximation holds for frequencies below 1 THz, where only acoustic modes are present.

From the frequency distribution it is easy to obtain the contribution of the external modes to the different thermodynamic functions. From statistical mechanics theory, for a harmonic crystal, the Gibbs potential is found to be

$$G = k_B T \sum_{\mathbf{q}} \sum_{j} \ln\{1 - \exp|-\hbar\omega_j(\mathbf{q})/k_B T|\} + \sum_{\mathbf{q}} \sum_{j} \hbar\omega_j(\mathbf{q})/2 + E_{\text{pack}} + pV,$$

where j stands for the different modes ($6Z$ for each wave vector $\mathbf{q}$), ω is the angular frequency, E_{pack} is the packing energy, k_B is the Boltzmann constant, T, p and V are temperature, pressure and volume, respectively. The sum over $\mathbf{q}$ can be replaced by introducing the factor $6NZ\,g(\omega)$, where $g(\omega)$ is the density of modes normalized to unity. For the vibration energy the following expression is obtained:

$$E_{\text{vib}} = \sum_{\mathbf{q}} \sum_{j} \frac{\hbar\omega_j(\mathbf{q})}{\{\exp[\hbar\omega_j(\mathbf{q})/k_B T] - 1\}} + \sum_{\mathbf{q}} \sum_{j} \hbar\omega_j(\mathbf{q})/2,$$

where the second term is the zero-point-motion energy.

* Figs. 3(a) and 3(b) have been deposited with the British Library Lending Division as Supplementary Publication No. SUP 39549 (3 pp.). Copies may be obtained through The Executive Secretary, International Union of Crystallography, 5 Abbey Square, Chester CH1 2HU, England.

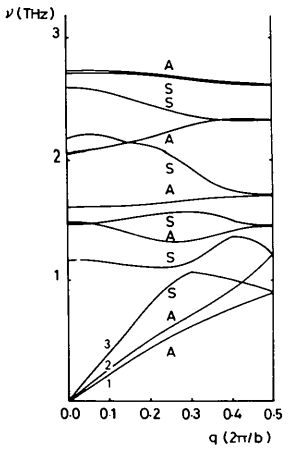

Fig. 2. Calculated dispersion curves along the b^* direction.

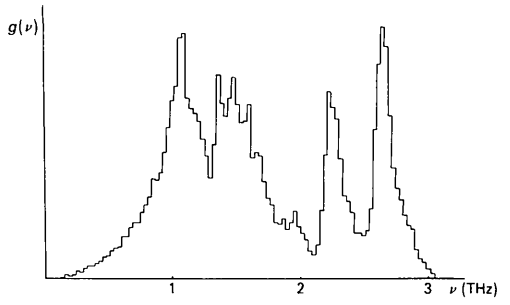

Fig. 3. Total external frequency distribution function.

The internal energy U can be obtained as $U = E_{vib} + E_{pack}$ and the entropy as $S = (U - F)/T$, where F is the Helmholtz free energy. The Ewald–Bertaut–Williams convergence method (Williams, 1971) has been utilized to eliminate cut-off effects in lattice sums ($-A/r^6$ long-range term, strictly speaking). Cut-off distances of 6 Å in direct space and 0·6 Å^{-1} in reciprocal space and a convergence constant of 0·27 have been assumed, giving a value of 6·17 kJ mol^{-1} with an estimated relative error of 10^{-4} with respect to the infinite limit in the lattice sums. The energy value obtained with a maximum distance of 6 Å in direct space represents 75% of the whole crystal energy. According to our calculations thermodynamic values at 300 K and 1 atm (1 atm = 0·1013 M Pa) are: $G = -7{\cdot}37$, $E_{vib} = 0{\cdot}86$, $U = 5{\cdot}31$ kJ mol^{-1} and $S = 6{\cdot}87$ J mol^{-1} K^{-1}. The term pV is negligible, so F and G values are the same. Results are rather insensitive to sampling density and a mesh of six points per axis yields identical values, probably due to the average character of thermodynamic functions over the Brillouin zone (see also Filippini & Gramaccioli, 1981). Unfortunately, we lack vibrational or thermodynamic experimental data for comparison with our results.

Thermal motion

The thermal vibration parameters are obtained experimentally in the crystal structure analysis. Tensors **T**, **L** and **S** (Schomaker & Trueblood, 1968) are defined to describe the mean rigid motion of molecules in the crystal. In terms of lattice dynamics they may be obtained with the following expressions (Willis & Pryor, 1975):

$$T_{\alpha\beta}(k) = N^{-1}\{m^t_\alpha(k)m^t_\beta(k)\}^{-1/2} \times \sum_j \sum_{\mathbf{q}} [E_j(\mathbf{q})/\omega_j^2(\mathbf{q})]\, e^t_\alpha(\mathbf{q}|kj) e^{t*}_\beta(\mathbf{q}|kj)$$

$$L_{\alpha\beta}(k) = N^{-1}\{m^r_\alpha(k)m^r_\beta(k)\}^{-1/2} + \sum_j \sum_{\mathbf{q}} [E_j(\mathbf{q})/\omega_j^2(\mathbf{q})]\, e^r_\alpha(\mathbf{q}|kj) e^{r*}_\beta(\mathbf{q}|kj)$$

$$S_{\alpha\beta}(k) = N^{-1}\{m^t_\alpha(k)m^r_\beta(k)\}^{-1/2} \times \sum_j \sum_{\mathbf{q}} [E_j(\mathbf{q})/\omega_j^2(\mathbf{q})]\, e^t_\alpha(\mathbf{q}|kj) e^{r*}_\beta(\mathbf{q}|kj),$$

where N represents the number of unit cells in the crystal, *i.e.* the number of allowed $\mathbf{q}$ vectors inside the Brillouin zone when boundary cyclic conditions are adopted, $E_j(\mathbf{q})$ the energy of the mode $(\mathbf{q}j)$ (k_BT, in the high-temperature limit), $e^t(\mathbf{q}|kj)$ and $e^r(\mathbf{q}|kj)$ represent the translational and rotational components relative to molecule k of the polarization vectors normalized to unity.

If the crystal has a finite size, the sums over the wave vectors inside the BZ can be expressed as integrals; their values may be obtained by dividing the BZ into volume elements and by approximating the integral over an element by the value of the integrand in its centre multiplied by its volume. Nevertheless, this method implies that the variation of the function through the field should be smooth. Actually, the frequencies of acoustic modes tend to zero for $q \to 0$, and the integrand becomes divergent, though the integral remains finite because the number of these modes also tends to zero when $q \to 0$. To overcome this problem two methods have been proposed: the first one (Filippini, Gramaccioli, Simonetta & Suffritti, 1976) uses non-uniform sampling with a greater density near the origin; and the second one an even sampling with an analytical evaluation of the integral over the element centred on the origin (Kroon & Vos, 1978). We have chosen the second method in which the origin element is surrounded by 26 volume elements, forming a large macrocube. These elements can be classified into three types: (*a*) centred on the faces of the macrocube; (*b*) centred on the edges; (*c*) centred on the vertices. If a linear behaviour of the acoustic branches through the macrocube is supposed, it is possible to obtain the contribution of the origin element from the contributions of the 26 elements, approximating the $q \to 0$ element by a sphere inscribed in it. We have found this contribution to be

$$I(q=0) = 0{\cdot}222 \sum_a I(a) + 0{\cdot}521 \sum_b I(b) + 0{\cdot}770 \sum_c I(c),$$

where the sums go through the elements of each type. However, these approximations introduce an error which can be corrected with an empirical factor η (Kroon & Vos, 1978) that multiplies the contribution of the $q \to 0$ element. This factor may be found by performing a numerical integration of the q^{-2} function in a sphere; we have seen that for samplings above 13 divisions per diameter $\eta = 1{\cdot}38$.

In this way we have proceeded to the calculation of the tensors **T**, **L** and **S** of rigid-body movement. Crystal symmetry has been taken into account to reduce the computation time using the information contained in all the molecules in the unit cell. A binary axis together with time-reversal symmetry reduces the sampling zone to $\frac{1}{4}$ of the Brillouin zone: $\mathbf{b}^*$ and $\mathbf{a}^*$

Table 2. *Rigid-body movement tensors expressed in the principal inertia axes of the molecule* (*a*) *Lattice dynamics*; (*b*) *Schomaker–Trueblood fit*

T in 10^{-4} Å^2, L in 10^{-4} rad^2, S in 10^{-4} rad Å.

	(*a*)			(*b*)		
	295	−30	10	398	−13	26
T		370	4		322	−23
			390			325
	25	4	−2	46	−30	30
L		18	1		33	−19
			73			49
	2	2	−5	(−14)	6	4
S	−8	−1	5	1	(−1)	−3
	−3	−13	−6	12	−13	(15)

positive sense and c* complete. Nevertheless, because of the uneven number of divisions in each axis (including the $q \rightarrow 0$ element), multiplicity of the different reciprocal planes and lines must be taken into account.

In Fig. 4 we present the convergence of the principal components of **T** and **L** calculated at 300 K, where $2n+1$ is the number of divisions of each reciprocal vector. Convergence is achieved very soon ($n \sim 6$) and is poorer for the **T** tensor because the modes with $q \rightarrow 0$, which are critical for convergence, are practically translational. In Table 2 we present the tensors **T**, **L** and **S** obtained at 300 K with 27 divisions per basic reciprocal vector and referred to the principal inertia axes of the molecule.

Discussion

Once the rigid-body tensors are known, we may obtain easily the individual adimensional thermal parameters β_{ij} (Willis & Pryor, 1975), which can be compared with the experimental ones. We have calculated an agreement factor, defined as usual by

$$R = \sum_i \sum_{j \geq i} |\beta_{ij}(\text{exp}) - \beta_{ij}(\text{cal})| \Big/ \sum_i \sum_{j \geq i} |\beta_{ij}(\text{exp})|.$$

In our case $R = 0{\cdot}14$, a value which is similar to those encountered in lattice dynamical calculations of thermal parameters in aromatic hydrocarbons (Filippini, Gramaccioli, Simonetta & Suffritti, 1973; Gramaccioli, Filippini & Simonetta, 1982; Gramaccioli & Filippini, 1983) and also some heterocylces (Filippini, Gramaccioli & Simonetta, 1981). We have also calculated a value

$$\Delta\beta = \sum_i \sum_{j \geq i} [\beta_{ij}(\text{exp}) - \beta_{ij}(\text{cal})] \Big/ \sum_i \sum_{j \geq i} \beta_{ij}(\text{exp})$$

whose value, equal to $-2{\cdot}1$, indicates an overall overvaluation of calculated with respect to experimental factors, which may be due to thermal diffuse scattering effects. Nevertheless, experimental thermal parameters are subject to a considerable error because of the random deviations of measured intensities, which are transmitted in the least-squares structure-refinement process, and also due to the thermal diffuse scattering contribution, which introduces a systematic error. Simultaneously, even in the case of reasonably rigid molecules, there always exists a small non-rigidity, and the least-squares-fitted tensors **T**, **L** and **S**, which best reproduce experimental individual parameters, include non-rigid effects in some way. Anharmonicity also introduces changes which cannot be predicted in the lattice dynamical model we have adopted.

Because of these reasons we think that it is not significant to obtain an R agreement factor between calculated lattice dynamical and experimental thermal parameters lower than the one found between

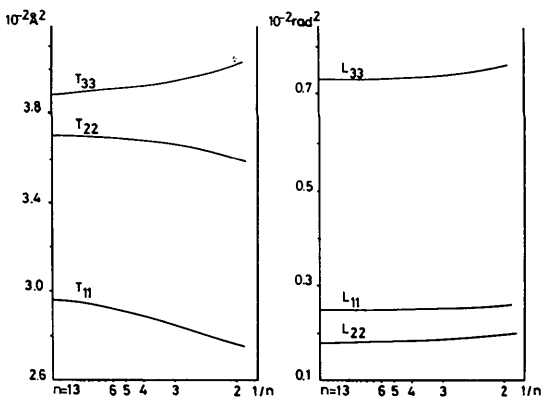

Fig. 4. Convergence of **T** and **L** rigid-body tensors.

Table 3. *Thermal crystallographic parameters* ($\times 10^4$)

$T = \exp -\{h^2\beta_{11} + k^2\beta_{22} + l^2\beta_{33} + 2hk\beta_{12} + 2hl\beta_{13} + 2kl\beta_{23}\}$.

		β_{11}	β_{22}	β_{33}	β_{12}	β_{13}	β_{23}
S	(*a*)	168 (2)	240 (4)	87 (1)	−64 (3)	15 (1)	38 (1)
	(*b*)	148	289	82	−38	37	8
	(*c*)	156	265	88	−34	25	32
N		192 (8)	217 (15)	10 (4)	−16 (8)	15 (5)	9 (6)
		162	211	86	1	36	−1
		175	192	83	−4	39	8
C(1)		154 (8)	239 (18)	92 (5)	18 (9)	30 (5)	−9 (7)
		149	348	81	−11	17	−12
		159	297	84	8	14	−6
C(2)		172 (10)	422 (23)	78 (5)	49 (13)	28 (6)	−4 (9)
		164	442	78	28	14	2
		159	396	75	51	22	0
C(3)		190 (10)	424 (23)	85 (5)	66 (13)	53 (6)	75 (9)
		186	425	83	50	26	45
		174	414	78	53	39	45
C(4)		164 (8)	281 (19)	106 (5)	18 (12)	43 (5)	61 (10)
		186	312	91	28	34	44
		185	312	87	17	42	51
C(5)		154 (8)	259 (16)	91 (5)	−30 (10)	38 (5)	−17 (3)
		159	310	85	−41	25	−17
		165	290	82	−40	30	−10
C(6)		147 (9)	394 (23)	77 (5)	−12 (11)	17 (5)	−15 (9)
		158	401	77	−16	18	−14
		153	362	73	−9	27	−14
C(7)		173 (9)	331 (19)	84 (5)	27 (15)	32 (5)	12 (11)
		180	374	71	26	21	11
		168	329	73	32	25	11
C(8)		183 (89)	224 (17)	72 (4)	0 (10)	38 (5)	10 (7)
		183	284	73	8	30	18
		179	255	81	10	23	27
C(9)		132 (7)	215 (13)	70 (4)	0 (9)	31 (5)	−4 (7)
		138	233	67	−1	36	0
		142	207	71	5	34	9
C(10)		144 (8)	214 (14)	75 (4)	6 (9)	33 (5)	−5 (7)
		136	228	72	−7	35	−10
		144	206	71	−4	38	−4
C(11)		136 (8)	227 (16)	85 (5)	23 (10)	28 (5)	12 (7)
		139	238	77	20	36	10
		148	216	74	18	41	16
C(12)		135 (8)	228 (15)	82 (5)	33 (9)	28 (5)	6 (9)
		124	261	73	3	31	−3
		135	223	74	12	31	5

(*a*) Experimental thermal parameters.
(*b*) Lattice dynamical thermal parameters.
(*c*) Thermal parameters obtained by rigid-body least-squares adjustment of the experimental ones.

experimental thermal parameters and those calculated from a least-squares fit of individual experimental parameters to a rigid model. To perform this analysis we have carried out a Schomaker–Trueblood fit over individual experimental parameters and the resulting **T**, **L** and **S** are shown in Table 2. We have recalculated from them the individual parameters, whose comparison with the experimental ones gives us an idea of their deviation from rigid-body behaviour. The agreement factor found is $R = 0{\cdot}116$, only slightly lower than the lattice dynamical result, so the lattice dynamical calculations are encouraging in view of the simplified hypothesis that we have adopted in our dynamical model.

In Table 3 experimental thermal parameters can be seen, together with lattice dynamical and Schomaker–Trueblood fit results.

The present work is part of a research programme supported by the Government through the Comisión Asesora de Investigación Científica y Técnica.

References

BELL, J. D., BLOUNT, J. F., BRISCOE, O. V. & FREEMAN, H. C. (1968). *Chem. Commun.* pp. 1656–1657.

BORN, M. & HUANG, K. (1954). *Dynamical Theory of Crystal Lattices.* Oxford: Clarendon.

BRADLEY, C. J. & CRACKNELL, A. P. (1972). *The Mathematical Theory of Symmetry in Solids.* Oxford: Pergamon Press.

BUSING, W. R. (1972). *Acta Cryst.* A **28**, S252–S253.

CHAPLOT, S. L., SAHNI, V. C. & RAO, K. R. (1981). *Acta Cryst.* A **37**, 374–377.

ESTRADA, M. D., CONDE, A. & MÁRQUEZ, R. (1983). *Acta Cryst.* B **39**, 739–742.

FILIPPINI, G. & GRAMACCIOLI, M. (1981). *Acta Cryst.* A **37**, 335–342.

FILIPPINI, G., GRAMACCIOLI, M. & SIMONETTA, M. (1981). *Chem. Phys. Lett.* **79**, 470–475.

FILIPPINI, G., GRAMACCIOLI, M., SIMONETTA, M. & SUFFRITTI, G. B. (1973). *J. Chem. Phys.* **59**, 5088–5101.

FILIPPINI, G., GRAMACCIOLI, M., SIMONETTA, M. & SUFFRITTI, G. B. (1976). *Acta Cryst.* A **32**, 259–264.

GRAMACCIOLI, M. & FILIPPINI, G. (1983). *Acta Cryst.* A **39**, 784–791.

GRAMACCIOLI, M., FILIPPINI, G. & SIMONETTA, M. (1982). *Acta Cryst.* A **38**, 350–356.

KROON, P. & VOS, A. (1978). *Acta Cryst.* A **34**, 823–824.

MASON, E. A. & RICE, W. E. (1954). *J. Chem. Phys.* **22**, 522–535.

MIRSKAYA, K. V. (1973). *Tetrahedron*, **29**, 679–682.

MIRSKAYA, K. V., KOZLOVA, I. E. & BEREZNITSKAYA, V. E. (1974). *Phys. Status Solidi B*, **62**, 291–294.

MIRSKAYA, K. V. & NAUCHITEL, V. V. (1971). *Sov. Phys. Crystallogr.* **16**, 891–892.

MIRSKAYA, K. V. & NAUCHITEL, V. V. (1972). *Sov. Phys. Crystallogr.* **17**, 56–59.

MIRSKY, K. (1978). *Computing in Crystallography*, edited by H. SCHENK, R. OLTHOF-HAZEKAMP, H. VAN KONINGSVELD & G. C. BASSI, pp. 169–182. Delft Univ. Press.

NETO, N. & KIRIN, D. (1979). *Chem. Phys.* pp. 245–250.

PAWLEY, G. S. (1970). *Crystallographic Computing*, edited by F. R. AHMED. Copenhagen: Munksgaard.

PAWLEY, G. S. (1972). *Phys. Status Solidi B*, **39**, 475–487.

SCHOMAKER, V. & TRUEBLOOD, K. N. (1968). *Acta Cryst.* B **24**, 63–76.

VENKATARAMAN, G. & SAHNI, V. C. (1970). *Rev. Mod. Phys.* **42**, 409–470.

WILLIAMS, D. E. (1967). *J. Chem. Phys.* **47**, 4680–4684.

WILLIAMS, D. E. (1971). *Acta Cryst.* A **27**, 452–455.

WILLIAMS, D. E. (1972). *Acta Cryst.* A **28**, 84–88.

WILLIS, B. T. M. & PRYOR, A. W. (1975). *Thermal Vibrations in Crystallography.* Cambridge Univ. Press.

Acta Cryst. (1984). A**40**, 701-703

Note on Strengthened Translation Functions: the Positioning of a Well Oriented Molecular Fragment Using *DIRDIF* Procedures

BY H. J. BRUINS SLOT AND PAUL T. BEURSKENS

Crystallography Laboratory, University of Nijmegen, Toernooiveld, 6525 ED Nijmegen, The Netherlands

(*Received* 10 *April* 1984; *accepted* 2 *July* 1984)

Abstract

Strengthened translation functions have been defined [Doesburg & Beurskens (1983). *Acta Cryst.* A**39**, 368–376] as convolutions of two electron density functions: *i.e.* the electron density representing the known fragment and the electron density obtained by the application of the *DIRDIF* procedures [Beurskens *et al.* (1982). In *Conformation in Biology*, edited by R. Srinivasan & R. H. Sarma. New York: Adenine Press]. Similar translation functions are defined as convolutions of the *DIRDIF* Fourier map with itself. The new functions are less powerful. The combination of the two types of functions, however, results in a more reliable method for the positioning of a fragment, if the fragment constitutes at least 10% of the total scattering power of the primitive unit cell. Examples of applications to known structures are given.

Introduction

The position of a correctly oriented fragment, represented by the electron-density function ρ_p, can be

0108-7673/84/060701-03$01.50